

DOI: [10.29026/oea.2025.240220](https://doi.org/10.29026/oea.2025.240220)CSTR: [32247.14.oea.2025.240220](https://cstr.org/cstr/32247.14/oea.2025.240220)

Tunable vertical cavity microlasers based on MAPbI₃ phase change perovskite

Rongzi Wang^{1†}, Ying Su^{1†}, Hongji Fan¹, Chengxiang Qi¹,
Shuang Zhang^{2,3,4} and Tun Cao^{1†*}

¹School of Optoelectronic Engineering and Instrumentation Science, Dalian University of Technology, Dalian 116024, China; ²New Cornerstone Science Laboratory, Department of Physics, University of Hong Kong, Hong Kong 999077, China; ³Department of Electrical & Electronic Engineering, University of Hong Kong, Hong Kong 999077, China; ⁴Materials Innovation Institute for Life Sciences and Energy (MILES), HKU-SIRI, Shenzhen 518052, China.

[†]These authors contributed equally to this work.

*Correspondence: T Cao, E-mail: caotun1806@dlut.edu.cn

This file includes:

Section 1: Complex refractive index of MAPbI₃ film at different temperatures

Section 2: Size distribution of crystals in MAPbI₃ thin films

Section 3: The surface roughness and height profile of each part of the VCSEL structure

Section 4: Characterization of MAPbI₃ film

Section 5: Measured PL spectra of MAPbI₃ layer at different temperatures

Section 6: Effect of perovskite film thickness on VCSEL PL spectra and relationship with spin speed

Section 7: The VCSEL laser emissions from 130 K to 160 K

Section 8: Laser performance of the VCSEL microlaser at 135 K, 140 K and 150 K

Supplementary information for this paper is available at <https://doi.org/10.29026/oea.2025.240220>



Open Access This article is licensed under a Creative Commons Attribution 4.0 International License.

To view a copy of this license, visit <http://creativecommons.org/licenses/by/4.0/>.

© The Author(s) 2025. Published by Institute of Optics and Electronics, Chinese Academy of Sciences.

Section 1: Complex refractive index of MAPbI₃ film at different temperatures

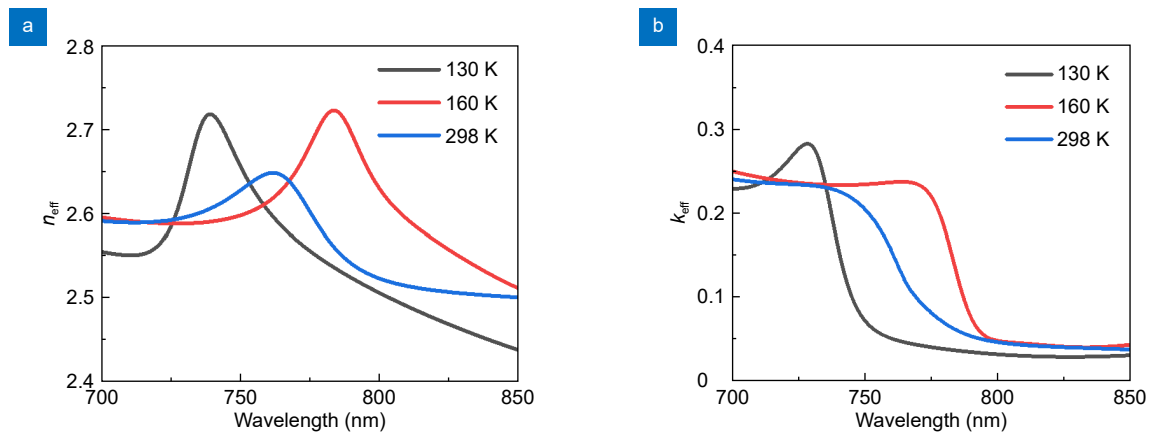


Fig. S1 | The complex refractive index of perovskite PCM (MAPbI₃) at the various temperatures. (a) Real part (n_{eff}) and (b) imaginary part (k_{eff}) of complex refractive index (N_{eff}) of 300 nm thick MAPbI₃ at the various temperatures.

Section 2: Size distribution of crystals in MAPbI₃ thin films

We conducted a statistical analysis of the size of crystals in MAPbI₃ films based on the SEM images. The detailed statistical data are shown in Fig. S2. It can be seen that about 72% of the particle size distribution is between 100 nm and 200 nm.

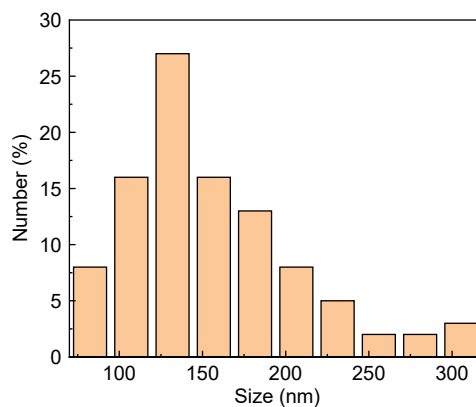


Fig. S2 | Size distribution of nanocrystals in MAPbI₃ thin films.

Section 3: The surface roughness and height profile of each part of the VCSEL structure

In Fig. S3, the surface roughness of DBR mirror grown on the quartz substrate was measured by the atomic force microscope (AFM, Park NX10). The scanned area was $30\ \mu\text{m}\times 30\ \mu\text{m}$, and the root-mean-square (RMS) value of the surface roughness was about 1.2 nm. Subsequently, the surface roughness of MAPbI₃ film coated on the DBR mirror was measured. The scanned area was also $30\ \mu\text{m}\times 30\ \mu\text{m}$, and the RMS value of surface roughness was about 4.1 nm. The surface roughness of the microcavity was obtained by measuring the gold layer growing on the MAPbI₃ film. The scanning area of the microcavity is still $30\ \mu\text{m}\times 30\ \mu\text{m}$, and the RMS value of the surface roughness is about 11.5 nm.

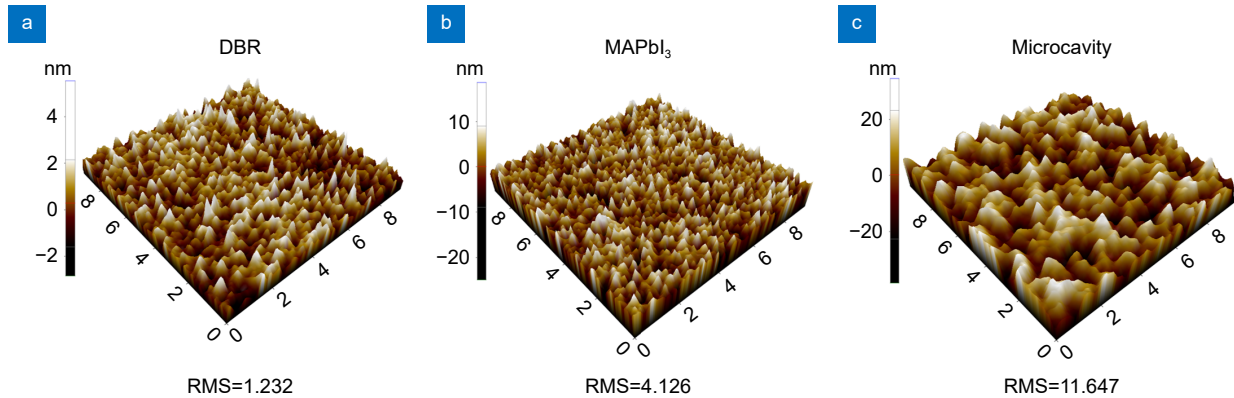


Fig. S3 | The experimentally measured surface roughnesses and height profiles of the (a) DBR mirror, (b) MAPbI₃ film and (c) microcavity structure, respectively.

Section 4: Characterization of MAPbI₃ film

Figure S4(a) presents an optical microscope image of an as-prepared MAPbI₃ film deposited on a quartz glass substrate. The MAPbI₃ film exhibits a smooth surface, which indicates excellent crystallinity of the nanocrystalline layer. Atomic force microscopy (AFM) and scanning electron microscopy (SEM) images are shown in Fig. S4(b) and S4(c), respectively, with the thickness of the film in the thinner regions measured at approximately 300 nm. The height profile suggests that the thickness of the MAPbI₃ film is uniform across the surface. Additionally, higher magnification SEM images (Fig. S4(c)) reveal that the synthesized MAPbI₃ perovskite exhibits clear nanocrystal (NC) characteristics, with grain sizes on the order of hundreds of nanometers. X-ray diffraction (XRD) is employed to characterize the MAPbI₃ film in its tetragonal and orthorhombic phases, as shown in Fig. S4(d). Upon heating from 130 K to 160 K, a significant change is observed, with the appearance of a new peak at $2\theta = 32.2^\circ$. As the temperature increases, the peak positions progressively shift toward lower angles. Simultaneously, the characteristic peaks of the tetragonal phase become more pronounced, while those corresponding to the orthorhombic phase decrease in intensity. The XRD peaks at $2\theta = 24.5^\circ$ (022), 33.6° (310), and 44.2° (116) remain unchanged throughout the phase transition. Between 190 K and 250 K, both the peak intensities and shapes remain relatively stable, suggesting that the tetragonal MAPbI₃ structure is stable within this temperature range, with no new phase transitions occurring and maintaining a high degree of crystallinity. During the phase transition, the narrowing of the peak widths indicates that the crystallinity of the tetragonal phase is superior to that of the orthorhombic phase.

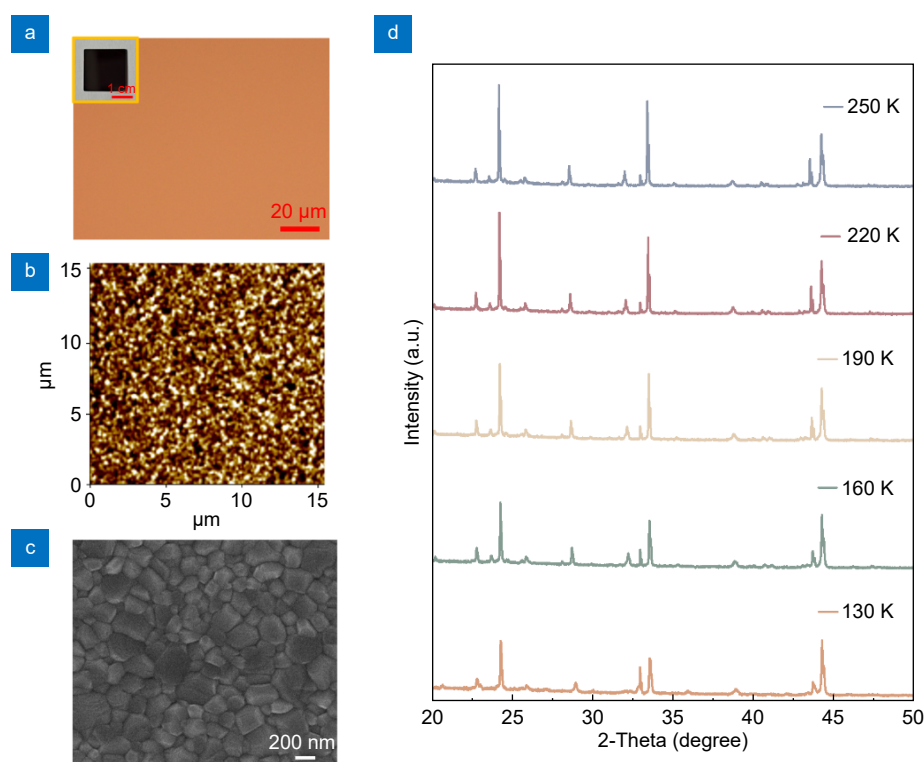


Fig. S4 | (a) Optical microscope, the inset is photograph of the MAPbI₃ film on the quartz glass substrate, Scale bar: 1 cm. (b) Atomic force microscope (AFM) and (c) SEM pictures of an exfoliated MAPbI₃ polycrystalline layer on the quartz glass substrate, respectively. (d) XRD spectra of the MAPbI₃ film from 250 K to 130 K (tetragonal (160 K) and orthorhombic (130K)).

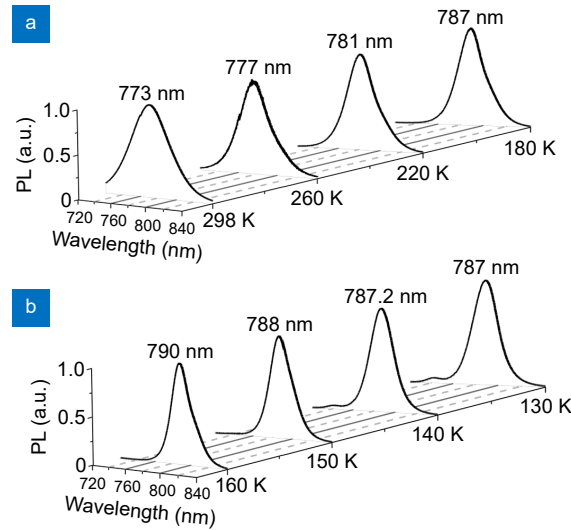
Section 5: Measured PL spectra of MAPbI₃ layer at different temperatures

Fig. S5 | Evolution of PL spectra from the MAPbI₃ layer (a) from 298 K to 180 K and (b) from 160 K to 130 K.

Section 6: Effect of perovskite film thickness on VCSEL PL spectra and relationship with spin speed

The thickness of the MAPbI₃ film significantly affects the performance and resonant mode of VCSEL. The sandwich structure comprising the DBR mirror, MAPbI₃ film, and Au film forms an F-P cavity. The weakly coupled perovskite F-P cavity laser operates as a photon laser, with its generation process progressing through spontaneous emission (SE), amplified spontaneous emission (ASE), and ultimately stimulated emission (STE). Consequently, it is essential to align the resonance mode of the F-P cavity with the ASE peak position of the MAPbI₃ film. To achieve this alignment for both the tetragonal and orthorhombic states of the MAPbI₃ films, we simulated the optimal thickness of the MAPbI₃ film to be approximately 300 nm, as illustrated in Fig. S6(a). To study the relationship between spin coating speed and thickness, we varied the thickness of the MAPbI₃ layer by the various spin speeds from 3000 rpm to 5500 rpm, as shown in Fig. S6(b).

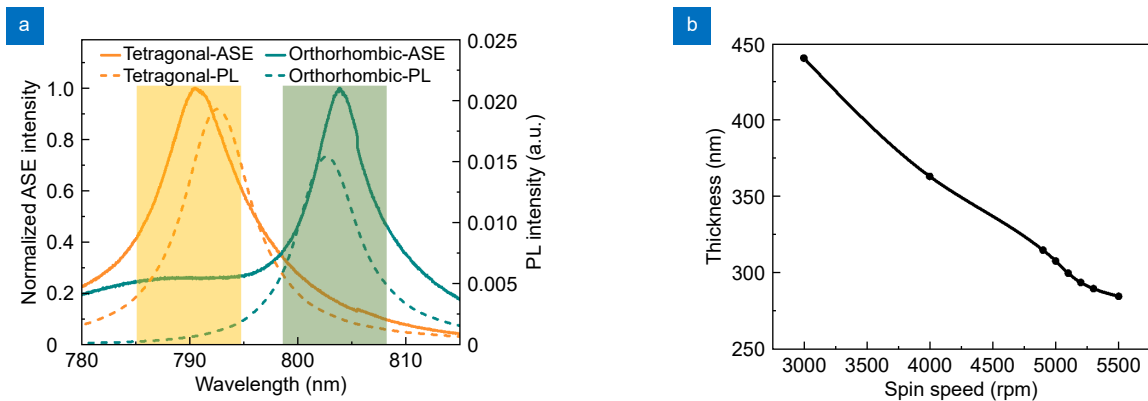


Fig. S6 | (a) The ASE spectra of a 300 nm perovskite layer and The PL spectra of a VCSEL structure with a 300 nm perovskite active layer. The yellow and green shaded areas are the ASE gain areas at the tetragonal and orthorhombic states respectively. (b) Different active perovskite layer thickness with the spin coating speed. Spin speed (x-axis) VS perovskite layer thickness (y-axis).

Section 7: The VCSEL laser emissions from 130 K to 160 K

The tuning rate was calculated based on the change in wavelength with respect to the change in temperature. For our VCSEL, when the temperature changes from 130 K to 160 K, the wavelength changes from 790.6 nm to 799.7 nm, as shown in Fig. S7. Plugging these values into the formula, we get: Tuning rate = $(799.7 - 790.6) / (160 - 130) \approx 0.30 \text{ nm K}^{-1}$, which validates the reported tuning rate.

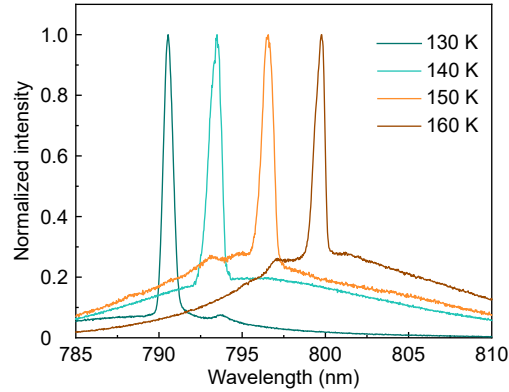


Fig. S7 | The emission spectrum of VCSEL at the various temperatures of 130 K, 140 K, 150 K and 160 K, respectively.

Section 8: Laser performance of the VCSEL microlaser at 135 K, 140 K and 150 K

The laser characteristics of MAPbI₃ VCSEL at 135 K, 140 K and 150 K were also studied by collecting the light emission in the backscattering configuration. The light emission spectra of the VCSEL under different pumping fluences are measured at 135 K and shown in the upper row of Fig. S8(a). A weak broad radiation spectrum is observed for $F_{\text{pump}} < 42 \mu\text{J cm}^{-2}$, at a larger fluence of $F_{\text{pump}} = 42.8 \mu\text{J cm}^{-2}$, a single narrow lasing emission peak appears at $\sim 792 \text{ nm}$. At 140 K and 150 K, the laser exhibits similar properties. The laser emission peak is located at about 793.5 nm, and the threshold is about $24.9 \mu\text{J cm}^{-2}$ at 140 K. At 150 K, the laser threshold is about $22.2 \mu\text{J cm}^{-2}$, and the laser emission peak center wavelength is about 796.5 nm.

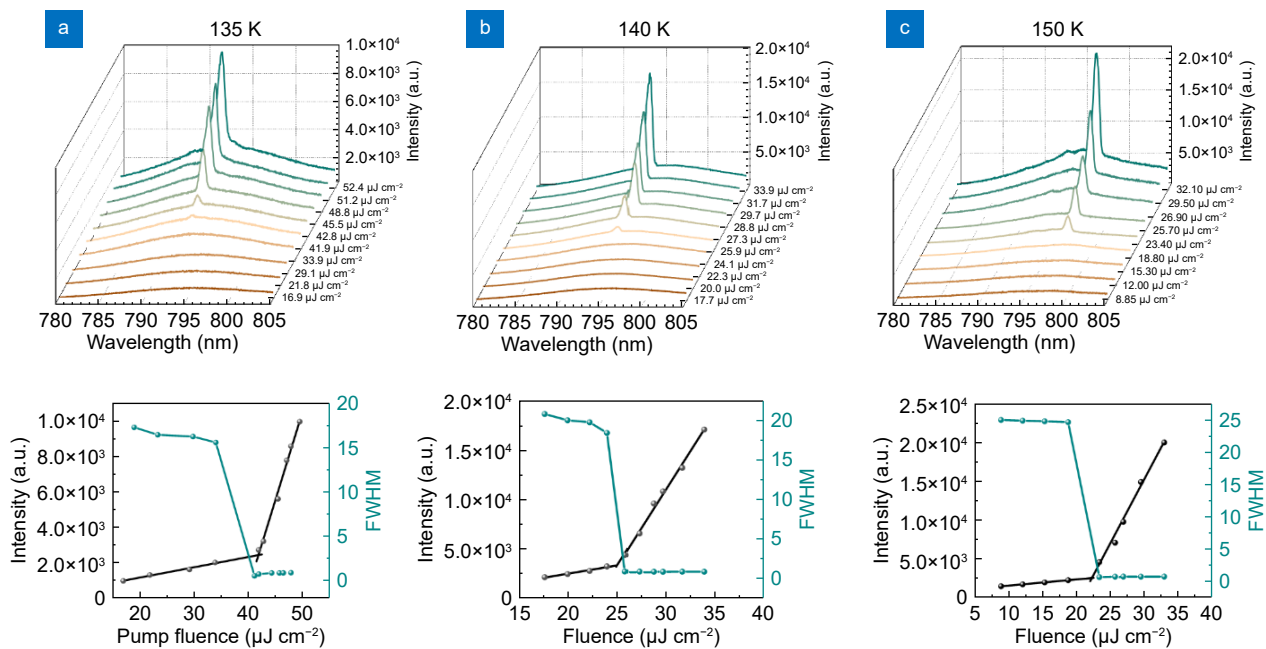


Fig. S8 | Laser performance of the VCSEL microlaser. (a–c) Emission spectra of the VCSEL against pump fluence at 135 K, 140 K, 150 K (upper row); light-light curve of the laser at 135 K, 140 K, 150 K (lower row).